Biochimica et Biophysica Acta 1798 (2010) 1779–1789

Contents lists available at ScienceDirect

Biochimica et Biophysica Acta

journal homepage: www.elsevier.com/locate/bbamem

Investigation of the interaction between modified ISCOMs and stratum corneum lipid model systems

Henriette Baun Madsen [a], Helle M. Arboe-Andersen [a,b], Noemi Rozlosnik [c], Flemming Madsen [d], Peter Ifversen [d], Marina R. Kasimova [a], Hanne Mørck Nielsen [a,*]

[a] Department of Pharmaceutics and Analytical Chemistry, Faculty of Pharmaceutical Sciences, University of Copenhagen, Universitetsparken 2, DK-2100 Copenhagen, Denmark
[b] Nordic Vaccine A/S, Fruebjergvej 3, DK-2100 Copenhagen, Denmark
[c] Department of Micro- and Nanotechnology, Technical University of Denmark, Ørsteds Plads, DK-2800 Kgs. Lyngby, Denmark
[d] Coloplast A/S, Bakkegårdsvej 406A, DK-3050 Humlebæk, Denmark

ARTICLE INFO

Article history:
Received 2 March 2010
Received in revised form 20 May 2010
Accepted 2 June 2010
Available online 11 June 2010

Keywords:
ISCOMs
Skin
Interaction
ITC
FRET
AFM
Drug delivery

ABSTRACT

The modified ISCOMs, so-called Posintro™ nanoparticles, provide an opportunity for altering the surface charge of the particles, which influences their affinity for the negatively charged antigen sites, cell membranes and lipids in the skin. Hypothetically, this increases the passage of the ISCOMs (or their components) and their load through the stratum corneum. The subsequent increase in the uptake by the antigen-presenting cells results in enhanced transcutaneous immunization. To understand the nature of penetration of Posintro™ nanoparticles into the intercorneocyte space of the stratum corneum, the interaction between the nanoparticles and lipid model systems in form of liposomes and/or supported lipid bilayer was studied. As a lipid model we used Stratum Corneum Lipid (SCL), a mixture similar in composition to the lipids of the intercorneocyte space. By Förster Resonance Energy Transfer (FRET), Atomic Force Microscopy (AFM), Electrochemical Impedance Spectroscopy (EIS) and cryo-Transmission Electron Microscopy (cryo-TEM) it was shown that application of nanoparticles to the SCL bilayers results in lipid disturbance. Investigation of this interaction by means of Isothermal Titration Calorimetry (ITC) confirmed existence of an enthalpically unfavorable reaction. All these methods demonstrated that the strength of electrostatic repulsion between the negatively charged SCL and the nanoparticles affected their interaction, as decreasing the negative charge of the Posintro™ nanoparticles leads to enhanced disruption of lipid organization.

1. Introduction

Immune-stimulating complexes (ISCOMs) represent a well-known type of adjuvant delivery system for vaccines. In microscopic images, ISCOMs appear as 40–60 nm spherical cage-like structures. They contain a large amount of the immunological adjuvant saponin (Quil A), as well as cholesterol and phospholipids. When mixed in proper proportions, these components spontaneously self-assemble into the negatively charged nanoparticles [1], to which antigens can be associated. The negative surface charge presents a challenge, since the ISCOMs are intended to associate to the negatively charged antigen sites [2] and the cell surface molecules, negatively charged as well. Therefore, attempts have been made to prepare positively charged ISCOMs (PLUSCOMs) for the use as vaccine adjuvants [2,3]. A new generation of ISCOMs, the Posintro™ nanoparticles [4,5], contains a positively charged cholesterol derivative, 3ß-[N-(*N'*,*N'*-dimethylaminoethane)-carbamoyl]cholesterol (DC-cholesterol), which is partly neutralizing the overall negative surface charge, and thus might increase the interaction with and subsequent uptake by antigen presenting cells (APCs).

Transcutaneous administration of vaccines is a potential alternative to injection. Immunizations through the skin, which is rich in APCs, is attractive because it is non-invasive, pain-free, non-traumatic for the patient, and does not require trained staff for proper administration. Furthermore, the large amount of APCs (Langerhans cells) present in the epidermis will be targeted by transcutaneous vaccination [6,7]. However, the targeting of vaccines to Langerhans cells is strongly dependent on the application of a delivery system, which can facilitate penetration of the antigen through the skin barrier and subsequently present the antigen to the APCs in the epidermis.

The main barrier for transcutaneous delivery is the outermost layer of the skin, the stratum corneum; a 5–20 µm thick layer consisting of dead degranulated keratin filled cells, the corneocytes, embedded in regions of mixed lipids. The intercorneocyte space in the

* Corresponding author. Department of Pharmaceutics and Analytical Chemistry, Faculty of Pharmaceutical Sciences, University of Copenhagen, Universitetsparken 2, Copenhagen, Denmark. Tel.: +45 3533 6346; fax: +45 3533 6030.
E-mail address: hmn@farma.ku.dk (H.M. Nielsen).

0005-2736/$ – see front matter © 2010 Published by Elsevier B.V.
doi:10.1016/j.bbamem.2010.06.006

stratum corneum is <20 nm [8], and the main lipid components are well known [9,10]. The major classes of lipids in the stratum corneum are ceramides, cholesterol and fatty acids. These lipids exist as intercellular lamellae with an orientation approximately parallel to the surface of the corneocytes [11,12]. Numerous approaches have been suggested for overcoming the barrier function of the stratum corneum. Some strategies aim at developing a drug delivery system which transiently increases the permeability of the skin, others are designed to bypass or even remove the outermost skin layer [13].

Cutaneous application of Posintro™ nanoparticles has been shown to enhance transcutaneous delivery of hydrophobic model compounds [14]. It was shown that a model compound incorporated into the Posintro™ nanoparticles penetrates into the epidermis through the intercorneocyte space in the stratum corneum, thus passing through the intercorneocyte lipids. However, the current consensus is that despite their small size, the nanoparticles are not able to squeeze between the corneocytes while staying intact. The hypothesis is therefore that the modified ISCOMs disturb the intercorneocyte lipid lamellae in the stratum corneum and thus enhance the penetration of the model compounds into the epidermis where the target cells reside [14].

The objective of the current study was to investigate interaction between modified ISCOMs with different surface charge and the lipids in the intercorneocyte space of the stratum corneum. The model used was Stratum Corneum Lipid Liposomes (SCLLs) and Stratum Corneum Lipid supported bilayer prepared from SCLL. SCLLs have previously been used in FRET studies to investigate the interaction between the skin and liposomes intended for drug delivery [15,16]. These studies indicated that the degree of interaction with SCLLs was dependent on the composition and structure of the nanoparticles.

In our work, interaction between Stratum Corneum Lipids and Posintro™ nanoparticles was analyzed by FRET, AFM, EIS and cryo-TEM techniques, whereas its thermodynamic characteristics were studied by ITC. In combination, these methods provide a deeper insight into the mechanism of interaction between the Posintro™ nanoparticles and the stratum corneum intercorneocyte lipids.

2. Experimental procedures

2.1. Materials

Quil A was obtained from Brenntag Biosector, Denmark and mega-10 (N-decanoyl-N-methylglucamide) was from Bachem, Germany. Cholesterol (>98%), DOPE (dioleyl phosphatidylethanolamine, >99%) and POPC (1-Palmitoyl-2-Oleoyl-*sn*-Glycero-3-Phosphocholine, >99%) were obtained from Avanti Polar Lipids, Alabama, USA. DC-cholesterol (~95%), palmitic acid, α-hydroxy fatty acid ceramide from bovine brain (>98%), non-hydroxy fatty acid ceramides from bovine brain (>99%), cholesterol sulfate, CHEMS (cholesteryl hemisuccinate), Triton X-100 and poly(DADMAC) (poly(diallyldimethylammonium chloride)) were obtained from Sigma-Aldrich. NBD-PE (*N*-(7-nitrobenz-2-oxa-1,3-diazol-4-yl)-1,2-dihexadecanoyl-*sn*-glycero-3-phosphoethanolamine) and Rh-DHPE (Lissamine™ rhodamine B 1,2-dihexadecanoyl-*sn*-glycero-3-phosphoethanolamine) were obtained from Invitrogen and methanol and chloroform from Merck. Phosphate-buffered saline (PBS) pH 7.4 was prepared from distilled, deionized water (Milli-Q Water system, Millipore, Billerica, MA, USA). Silicon (001) wafers were from Okmetic (Vantaa, Finland) and AHS (N-(6-aminohexyl)aminopropyltrimethoxysilane) from ABCR GmbH, Karlsruhe Germany and had a contact angle of 61°. Ethane and nitrogen was from AGA Gas AB (Sweden).

2.2. Methods

2.2.1. Preparation and characterization of Posintro™ nanoparticles

Posintro™ nanoparticles were prepared by the standard dialysis method first described by Höglund et al. in 1989 [17]. Briefly, cholesterol, DC-cholesterol and POPC were dissolved in 20% (w/v) mega-10 in Milli-Q water. The saponin, Quil A, was dissolved in Milli-Q water and appropriate amounts of the components were mixed and stirred for 2 h at 37 °C. The weight ratio between Quil A:POPC:total cholesterol was 5:1:1 and the total lipid concentration was 0.2% (w/v) before dialysis. Three types of particles with the same total amount of cholesterol, but with varying ratios of cholesterol:DC-cholesterol were prepared: particles without DC-cholesterol (Posintro™ 0%), particles with 25% of the cholesterol replaced by DC-cholesterol (Posintro™ 25%) and particles with 50% of the cholesterol replaced by DC-cholesterol (Posintro™ 50%). The mixtures were dialyzed in 10 kDa MW cut-off dialysis Slide-A-Lyzer® cassettes purchased from Thermo Fisher Scientific (Waltham, MA, USA). The dialysis in PBS pH 7.4 was performed for 64 h at 26 °C and subsequently for 48 h at 5 °C, the buffer was changed every 24 h in order to remove Mega-10, unincorporated Quil A and unincorporated lipids. Determination of density was performed in a discontinuous sucrose gradient with fractions of 50%, 40%, 30%, 20%, and 10% (w/v) sucrose. The samples were centrifuged for 4 h at 112,000*g* and 15 °C. Size distribution was measured by dynamic light scattering (DLS) (Zetasizer Nano ZS, Malvern, UK) in undiluted samples in small volume cuvettes. The size was stated as an average of four measurements. Zeta potential was measured by laser-Doppler electrophoresis (LDE) (Zetasizer Nano ZS, Malvern, UK) in 1/10 diluted PBS samples in Milli-Q water. The zeta potential was stated as an average of ten measurements. The Helmoholtz–Smoluchowski equation was used to convert the electrophoretic mobility to the zeta potential and the Malvern software was used for data acquisition and analysis using appropriate standards for size and zeta potential measurements. Furthermore, the surface charge of the Posintro™ nanoparticles was characterized by titration with a positively charged polymer, poly(DADMAC), as previously described in the literature [18,19].

2.2.2. Calculation of surface charge

The mobility of the nanoparticles was plotted against the charge density of the added polymer. The point, where the mobility of the nanoparticles equals zero, was used for determination of the charge density (C_d). Following that, the surface charge of the nanoparticles, Z, was determined with the equations below.

$$Z_{\text{nanoparticle}} = \frac{C_d \cdot m_p \cdot N_A}{n_p} \tag{1}$$

$$Z_{\text{area}} = \frac{Z_{\text{nanoparticle}}}{A_p} \tag{2}$$

The charge can be calculated per nanoparticle (Eq. (1)) or per nm^2 of the surface area (Eq. (2)), m_p is the total mass of nanoparticles, N_A is Avogadro Constant, A_p is the surface area per nanoparticle. The total number of nanoparticles, n_p, was calculated as:

$$n_p = \frac{C_p}{(V_p - V_i)\cdot S\cdot \rho} \tag{3}$$

Where C_p is the concentration of Posintro™ 25% components (0.79 mg/ml, Table 1), V_p is the volume of a spherical particle calculated from the diameter measured by DLS (45.7 nm, see Table 1), V_i is the inner volume of the particle calculated from the estimated thickness of the lipid shell of the nanoparticles of 4.4 nm (unpublished data), ρ_p is the density of the nanoparticles (1139 kg/m^3, estimated by ultracentrifugation). Parameter S accounts for the fact that the surface of the nanoparticles has n holes. It is expressed as:

$$S = 1 - \frac{n\cdot r_{\text{hole}}^2}{4\cdot r_{\text{particle}}^2} \tag{4}$$

Table 1
Characteristics of Posintro™ nanoparticles.

Posintro™	Size[a] (nm) (polydispersity)	Components of nanoparticles	Concentration (mg/ml)	Zetapotential[b] (mV) (Z_{area}) (negative charges/nm^2)
0%	47.6 ± 0.4 (0.07 ± 0.02)	Quil A	0.67	−37 ± 13 (2.02)
		POPC	0.09	
		Cholesterol	0.12	
		DC-cholesterol	0.00	
		Total	**0.89**	
25%	45.7 ± 0.7 (0.09 ± 0.02)	Quil A	0.57	−33 ± 11 (1.34)
		POPC	0.09	
		Cholesterol	0.07	
		DC-cholesterol	0.05	
		Total	**0.79**	
50%	42.7 ± 0.5 (0.01 ± 0.00)	Quil A	0.53	−21 ± 7 (0.98)
		POPC	0.07	
		Cholesterol	0.03	
		DC-cholesterol	0.10	
		Total	**0.73**	

[a] Z-average of four DLS measurements (mean ± SD).
[b] Average of ten LDE measurements (mean ± SD).

The number of holes is estimated to be 20, the radius of the hole is 4 nm [20] and $r_{particle} = 22.85$ nm (Table 1). Substituting these values, we find that $S = 0.85$ and the number of the nanoparticles per liter is 3.5×10^{16}.

2.2.3. Concentration determination by HP-TLC

The exact lipid concentration of Posintro™ nanoparticles was determined by high performance thin layer chromatography (HP-TLC) using a cholesterol:DC-cholesterol:POPC mixture in the ratio 1:1:6 as a standard. The concentration range of the standard curve was 0.027–0.22 mg/ml for the cholesterols and 0.16–1.33 mg/ml for POPC. The standard curve obtained was linear in this range. The concentration of Quil A in the Posintro™ nanoparticles was also determined by HP-TLC. The standard curve was linear within the concentration range of 0.24–0.97 mg/ml. All samples were applied without preparation and all samples were within the limits of the standard curve.

Separation of the lipids was achieved on HP-TLC silica gel 60 (Merck) with chloroform, methanol, water, ammonia (71.7:26.4:1.3:0.6) (%) in a manner slightly modified from previously described [21]. The chromatograms were first stained with 10% copper sulfate in phosphoric acid for cholesterol and DC-cholesterol detection and then with iron (III) chloride for POPC detection. Separation of Quil A from the lipids was achieved on HP-TLC silica gel 60 (Merck) with chloroform, methanol and water (44:44:12) (%) containing 2.2% (w/v) calcium chloride dehydrate [22]. The chromatograms were stained with 50% sulfuric acid in methanol [23]. After each staining, the chromatograms were scanned and the spots of lipids or Quil A were analyzed by QuantiScan image software.

2.2.4. Preparation of stratum corneum lipid liposomes (SCLLs) and DOPE/CHEMS liposomes

The stratum corneum lipid liposomes (SCLLs) and the DOPE/CHEMS liposomes were prepared by methods slightly modified from those previously described [15]. The SCLLs were composed of non-hydroxy fatty acid ceramides, α-hydroxy fatty acid ceramides, cholesterol, palmitic acid and cholesterol-3-sulfate in a weight ratio of 25:15:25:25:10. In addition, the lipid mixture used for the FRET studies contained 1 mol% of Rh-DHPE and 1 mol% of NBD-PE. Briefly, the lipids were dissolved individually in a mixture of chloroform: methanol (ratio 2:1), mixed and dried using a rotary evaporator. The lipid film was rehydrated with the help of ultrasound after adding small glass beads and 2.5 ml PBS pH 7.4. The mixture was extruded ten times through 100 nm polycarbonate filters (Nucleopore track-etched membrane, Whatman, UK) at 80 °C. Finally, PBS pH 7.4 was added to a total volume of 2.5 ml. The unincorporated fluorescent probes as well as free lipids in the resulting liposome suspension were removed by two column chromatography on Sephadex G-50 gel equilibrated with PBS pH 7.4. The size of the liposomes was determined by DLS (Zetasizer Nano ZS, Malvern, UK). For the FRET and the EIS studies 15 mg of lipid were used, whereas 75 mg of lipid were used for the ITC studies. The concentration of cholesterol in the SCLLs was measured by HP-TLC in the same way as for the Posintro™ nanoparticles. Based on these data, the total concentration of lipids was calculated under the assumption that the loss during preparation was similar for all lipids used for the SCLL.

The liposomes used as a reference (DOPE/CHEMS) were composed of DOPE and CHEMS in a weight ratio of 3:2. DOPE and CHEMS were dissolved individually in chloroform:methanol (2:1) and mixed. 15 mg of the lipid mixture was dried using a rotary evaporator. The lipid film was resuspended with ultrasound in 3 ml of PBS pH 7.4 for 30 min and sonicated for 10 min. After preparation, the size of the liposomes was measured using DLS (Zetasizer Nano ZS, Malvern, UK).

2.2.5. Förster Resonance Energy Transfer (FRET)

To prepare samples for the fluorescence measurements, 180 μl of NBD/Rh double-labeled SCLLs were diluted with 10 ml PBS and mixed for 5 min. Then, 200 μl of the diluted liposome suspension was added to a 96 well plate with transparent bottom (Thermo Fisher Scientific, USA). The plate was shaken in a FLUOstar OPTIMA plate-reader (BMG LABTECH, Offenburg, Germany) for 1 min and the initial fluorescence of the donor probe NBD was measured (excitation 485 nm and emission 535 nm) from the bottom of the plate. 10 μl of the test formulation (DOPE/CHEMS liposomes, Posintro™ nanoparticles or PBS pH 7.4) was added, the plate was shaken for 1 min and the fluorescence was measured every minute for the first 5 min and following every 5 min for 30 min with shaking for 1 min prior to each measurement. At the end of the experiment, the liposomes were disrupted by addition of 5 μl 4% (v/v) Triton X-100 solution and the plate was shaken. The values obtained in the presence of Triton X-100 were corrected for the effect of Triton X-100 (factor 1.25) [24] and dilution, and set to 100%. The results were expressed as a percentage of the maximum fluorescence as previously reported [15]. Measurements were performed in buffers of pH 7.4 and at 25 °C; each measurement was done at least in quadruplicate.

2.2.6. Isothermal Titration Calorimetry (ITC)

High-sensitivity titration calorimetry was used to study interaction between SCLLs and Posintro™ nanoparticles with different concentrations of DC-cholesterol. The experiments were performed by injecting the undiluted liposomes into the nanoparticle suspensions. The obtained thermodynamic parameters were compared to the ones observed with DOPE/CHEMS liposomes. The studies were performed on a Nano ITC instrument (TA Instruments, New Castle, DE, USA) with an active cell volume of 0.988 ml. Posintro™ nanoparticles or DOPE/CHEMS liposomes were titrated with SCLLs using an injection volume of 5 to 10 μl. The content of the reaction cell was stirred continuously at 300 rpm. The time interval between the injections was set to 5–10 min, allowing a complete equilibration of the system between the injections. Reference experiments, where the liposomes were injected into the buffer, or a buffer was injected into the solution of nanoparticles produced constant, non-zero heats. Titrations were done at 5 °C, 15 °C, 25 °C and 37 °C. Most of the experiments were performed twice.

2.2.7. ITC data analysis

Baseline subtraction and peak integration were done using Nano-Analyze software, following the standard procedure provided with the instrument. The data fitting, using the standard binding equations and a nonlinear least-squares fitting routine, was done in Excel

(Microsoft Corp, Redmont, WA, USA) using the model, where all binding sites are identical and independent. In addition to the usual thermodynamic parameters, such as enthalpy, ΔH, number of binding sites, n, and the binding constant, k, the residual heat, q_{off}, was fitted as well. This is the heat, associated with the dilution effects, observed at the end of titration experiment.

The reproducibility of the ITC experiments was much lower than expected. Knowing that the heat detection error per injection is less than 1 μcal, we estimated the influence of this error on the experimentally determined parameters. The calculated enthalpy changed within 5%, which was an order of magnitude lower than the largest observed difference between two runs performed with Posintro™ 50% (see Section 3). Therefore, the large errors are not associated with the ITC performance, but rather due to the investigated system. One possible source of poor reproducibility of the ITC titration is minor batch to batch variations, which cannot be observed in the DLS measurements. Another, more significant reason for the lack of reproducibility of the binding data is the presence of irreversible processes. Since such processes cannot be controlled, further reproducibility tests were abandoned and the averaging of the data was not performed. Furthermore, we would like to stress that the results must be considered as trends, rather than the processes with the defined characteristics or values, such as, in case of ITC, the precise thermodynamic parameters. Therefore, the observed clear trends in the thermodynamic parameters allow interpretation of the studied interactions.

As a rule, all fitting parameters were floated simultaneously. However, due to the non-sigmoidal shape of the titration curves, which made it difficult to evaluate the correct number of binding sites, the value for n was allowed to float only in a limited region, $n<2$. The top limit value was chosen, because in most cases, floating n produced numbers below 2. Where it did not, the fitting was not significantly improved by letting n settle at high numbers. It is important to note that in this treatment; n is the amount of moles of nanoparticle components bound per mole of SCLL components.

2.2.8. Estimation of particle molar concentrations for ITC analysis

The number of particles, both nanoparticles and liposomes, was estimated from their size (measured by DLS), density (ultracentrifugation) and the concentrations of the components, determined by HP-TLC as described above (Section 2.2.2, Eqs. (3) and (4)). The number of nanoparticles per liter, 3.5×10^{16}, was normalized by Avogadro's constant to obtain the molar concentrations of particles, resulting in molar concentration of Posintro™ 25% of approximately 5.7×10^{-5} mM. The densities of Posintro™ 0% and Posintro™ 50% nanoparticles were not measured and accordingly the number of the particles was not estimated. However, as the only difference between the nanoparticles is the ratio of DC-cholesterol/cholesterol, the density values of these nanoparticles, and thus their amounts, are expected to be similar to the one for Posintro™ 25%.

The same approach (Eq. (3)) was used to calculate the number of SCLL liposomes per liter. Parameters used for this calculation were: the radius of the liposomes (64 nm, from DLS measurements), the concentration of lipids in the suspension (4.13 g/l, HP-TLC), and the density of the particles (998 kg/m^3, obtained by ultracentrifugation). The concentrations of SCLL were calculated from the concentration of cholesterol measured by HP-TLC assuming that the lipids were equally distributed in the liposomes and therefore that the loss during production was similar for all lipids. According to the AFM data (see below) the thickness of the liposome bilayer was 5 nm, which is consistent with other reports [25]. Thus, the molar concentration of SCLL liposomes was estimated to 2.9×10^{-5} mM.

2.2.9. Electrochemical Impedance Spectroscopy (EIS)

The EIS analysis was completed with a VersaSTAT 3 instrument (Princeton Applied Research, TN, USA) and impedance chips. The chips were individually prepared and had a micro channel on top of a set of interdigitating electrodes consisting of the conducting polymer PEDOT (poly(3,4-ethylenedioxythiophene)) [26,27]. The design allows determination of the impedance of liquid samples injected into the micro channel.

The micro channel was flushed and filled with PBS pH 7.4 and the initial impedance was measured in a range of 0.32–100,000 Hz for 30 min. The PBS was replaced with SCLLs and the impedance measured for 90 min during which a lipid bilayer was formed. The formation of the lipid bilayer on the micro channel was confirmed by AFM prior to the experiments (data not shown). The excess lipid was removed by flushing the micro channel with PBS pH 7.4 (20 μl/min) and the impedance was measured for another 30 min. Then, Posintro™ nanoparticles, PBS pH 7.4 or DOPE/CHEMS liposomes were added to initiate the reaction with the lipid bilayer and the impedance was monitored for another 90 min. Finally, the system was flushed with PBS pH 7.4 and the impedance was measured for an additional 30 min. Each measurement was done at least in duplicate.

2.2.10. Atomic Force Microscopy (AFM)

For the AFM measurements, Si wafers coated with amino-silane monolayer were used. Clean Si wafers were immersed into a solution containing 2.5% (v/v) AHS and 2.5% (v/v) Milli-Q water in 2-propanol for 3 h. The deposition process was terminated by taking out the samples and rinsing them immediately in vast amount of 2-propanol, which was followed by successive rinsing in 2-propanol, 1:1 water/ethanol mixture and Milli-Q water. The AHS surface was dried by Argon gas. The quality of the silane monolayers was validated by AFM (data not shown). The roughness of the surfaces was less than 0.3 nm.

AFM investigations were performed with a PSIA XE 150 microscope (Park Systems, Suwon, Korea) in true-non-contact mode in liquid cell using Silicon tips (Multi75Al, BudgetSensors, with a resonant frequency 75 kHz, force constant 3 N/m). First the samples were imaged in PBS, and then 40 μl undiluted SCLLs was added to the PBS and mixed gently on the AHS-wafer by the pipette. Then the surface was continuously scanned and imaged for 2 h or until a flat lipid bilayer was formed. Before introduction of Posintro™ nanoparticles, the excess lipid was gently removed by repeated exchange of small volumes of the buffer. To investigate the interaction of the nanoparticles with the lipid bilayer, 50 μl of Posintro™ suspension were introduced to the sample. After 15 min equilibration time images were taken for 2 h.

2.2.11. Cryo Transmission Electron Microscopy (Cryo-TEM)

The SCLLs, Posintro™ nanoparticles and their mixtures similar to the ones obtained during calorimetric analysis were prepared in a controlled environment at 29 °C with a relative humidity kept close to saturation to prevent water evaporation from the sample. A 5-μl drop of the sample was placed on negatively charged coated lacey carbon film copper grids and excess liquid was removed by careful blotting with absorbent filter paper leaving thin (<300 nm) biconcave liquid films spanning the holes of the carbon grid. The sample was rapidly plunged into liquid ethane (−180 °C) and cooled by liquid nitrogen to obtain a vitrified film. The vitrified sample was stored under liquid nitrogen and transferred in a cryoholder (Oxford CT3500) and its workstation was used to transfer the specimen into the electron microscope (Philips CM120 BioTWIN Cryo) equipped with a post-column energy filter (Gatan GIF100). The acceleration voltage was 120 kV. The images were recorded digitally with a CCD camera under low electron dose conditions.

3. Results

3.1. Characterization of the Posintro™ nanoparticles and SCLLs

All particle batches were characterized by size and zeta potential. The concentrations of the components in the Posintro™ nanoparticles

were measured by HP-TLC (Table 1). For all types of Posintro™ nanoparticles the size range, between 40 and 50 nm, corresponded to the expected ISCOM structure size (Table 1) [1]. The polydispersity was low (i.e. <0.1), indicating a homogeneous size distribution in all preparations. The reproducibility of the preparation method was confirmed by a low inter-batch variability as evaluated by DLS size measurements. Furthermore, the cage-like structure of the nanoparticles was confirmed by cryo-TEM images (Fig. 9B–D). Measurements of the zeta potential by LDE and titration experiments indicated that increasing the amount of DC-cholesterol in the Posintro™ nanoparticles decreased their overall negative surface charge (Table 1). Thus, more cationic polymer was added with decreasing amounts of DC-cholesterol to obtain a mobility of zero (Fig. 1). This resulted in a decreasing number of negative charges per nm^2 (Eqs. (1–4)) with increasing amount of DC-cholesterol in the nanoparticles (Table 1).

The total concentration of components was 0.89 mg/ml for Posintro™ 0%, 0.79 mg/ml for Posintro™ 25% and 0.73 mg/ml for Posintro™ 50% (Table 1). From these results it can be observed that the amount of DC-cholesterol relative to cholesterol is higher than the theoretical value for both Posintro™ 25% and Posintro™ 50%.

The measured size of the SCLLs was 127 ± 10 nm and no obvious batch to batch variation was observed in the DLS size measurement. The total lipid concentration of SCLLs was 10.0 ± 0.1 mM, equal to 4.13 mg/ml.

In summary, the characterization of Posintro™ nanoparticles and SCLLs showed a good reproducibility of our preparation methods, confirmed by DLS size measurements. Furthermore, the overall negative surface charge of the Posintro™ nanoparticles decreased, as expected with increasing percentage of DC-cholesterol.

3.2. FRET-detected association of SCLLs

Fluorescence of SCLLs labeled with a donor-acceptor pair was used to monitor the interaction of Posintro™ nanoparticles with stratum corneum lipids. Upon mixing of the nanoparticles with the liposomes the donor fluorescence increased by 2–6% depending on the type of nanoparticles (Fig. 2). Similar studies were conducted at pH 5.5 with comparable results for the Posintro™ nanoparticles. However the DOPE/CHEMS liposomes showed a pH sensitive fusion behavior, as the increase in fluorescence was higher at pH 5.5 compared to pH 7.4 (data not shown). The reference DOPE/CHEMS liposomes gave rise to a 4% increase in fluorescence, whereas the negative control, PBS buffer, resulted in a small increase, ~0.5%. The data presented in Fig. 2 are consistent with the expectation that interaction between ISCOMs and SCLLs increases when the negative charge of the Posintro nanoparticles is decreased.

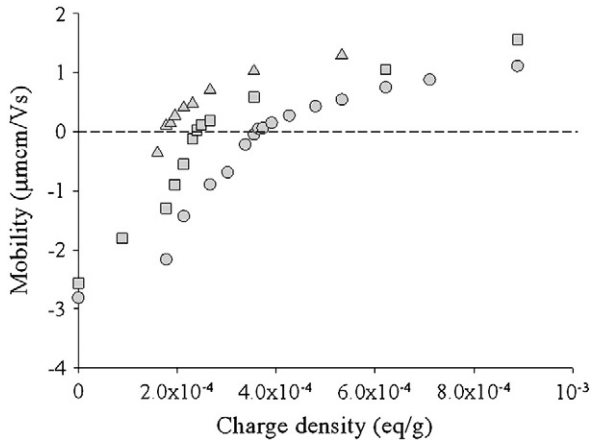

Fig. 1. Mobility of Posintro™ nanoparticles after addition of various amounts of cationic polymer (up triangles) Posintro™ with 0% DC-cholesterol, (squares) Posintro™ with 25% DC-cholesterol, (circles) Posintro™ with 50% DC-cholesterol.

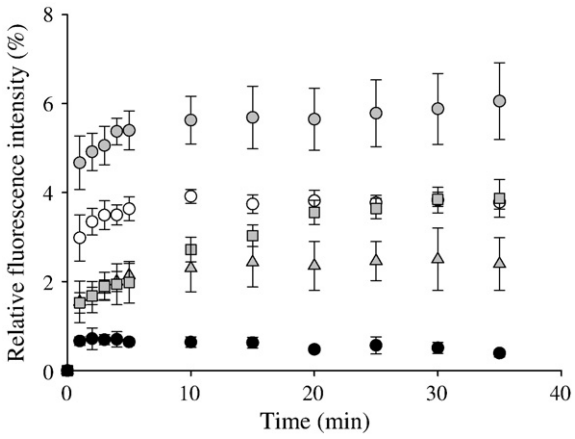

Fig. 2. Fluorescence of the double-labelled SCLLs upon addition of Posintro™ nanoparticles at pH 7.4. Each data point represents the average of 4 measurements ± standard deviation (open circles) DOPE/CHEMS-liposomes (reference), (up triangles) Posintro™ with 0% DC-cholesterol, (squares) Posintro™ with 25% DC-cholesterol, (circles) Posintro™ with 50% DC-cholesterol and (black circles) PBS.

3.3. Investigation of the SCLL surface by AFM

For the results reported, the formation of an intact stratum corneum lipid bilayer supported by the hydrophilic AHS surface occurred spontaneously and was completed within 70 min (Fig. 3). The thickness of the lipid bilayer was around 4–5 nm (see cross profile in Fig. 3), consistent with the expected value [25].

The integrity of the lipid surface after application of Posintro™ nanoparticles was followed as a function of time (Fig. 4, panels B and C). The texture of the surface became less and less rough over time, which indicates that the initial disturbance caused by the nanoparticles disappeared. No intact particles or partly flattened particles were seen on top of the bilayer indicating that the penetration into the lipid phase occurred already within the 15 min equilibration time (in which the samples were not scanned).

3.4. Thermodynamic studies of the binding between nanoparticles and liposomes

Interaction between the various Posintro™ nanoparticles and SCLLs was endothermic at all temperatures, indicating that the process was entropy-driven (Fig. 5A). The thermodynamic parameters for this interaction are summarized in Table 2. At the beginning of some experiments, a downturn of the titration curve was observed (Fig. 5B), indicating a presence of some other exothermic reaction. Since this effect was not always present, even in the same system, it could not be correlated to either the type of nanoparticles or the experimental temperature. Most probably this phenomenon was related to an incomplete balance between the buffers in the syringe and in the reaction cell or to minor batch to batch variations in nanoparticle preparation not detected by DLS measurements. Since, this exothermic reaction could not be controlled, it was not considered in the data treatment. This was done by excluding those injections that produced lower heat than the consecutive ones (for example, points 1 and 2 on the top curve of Fig. 5B were excluded from the fitting procedure).

The titration curves of the three types of Posintro™ nanoparticles with SCLLs at 25 °C are summarized in Fig. 5B. One trend that is clear from this graph is that the reaction becomes increasingly endothermic with the increase of DC-cholesterol content. The same effect is observed for different types of Posintro™ nanoparticles with increasing

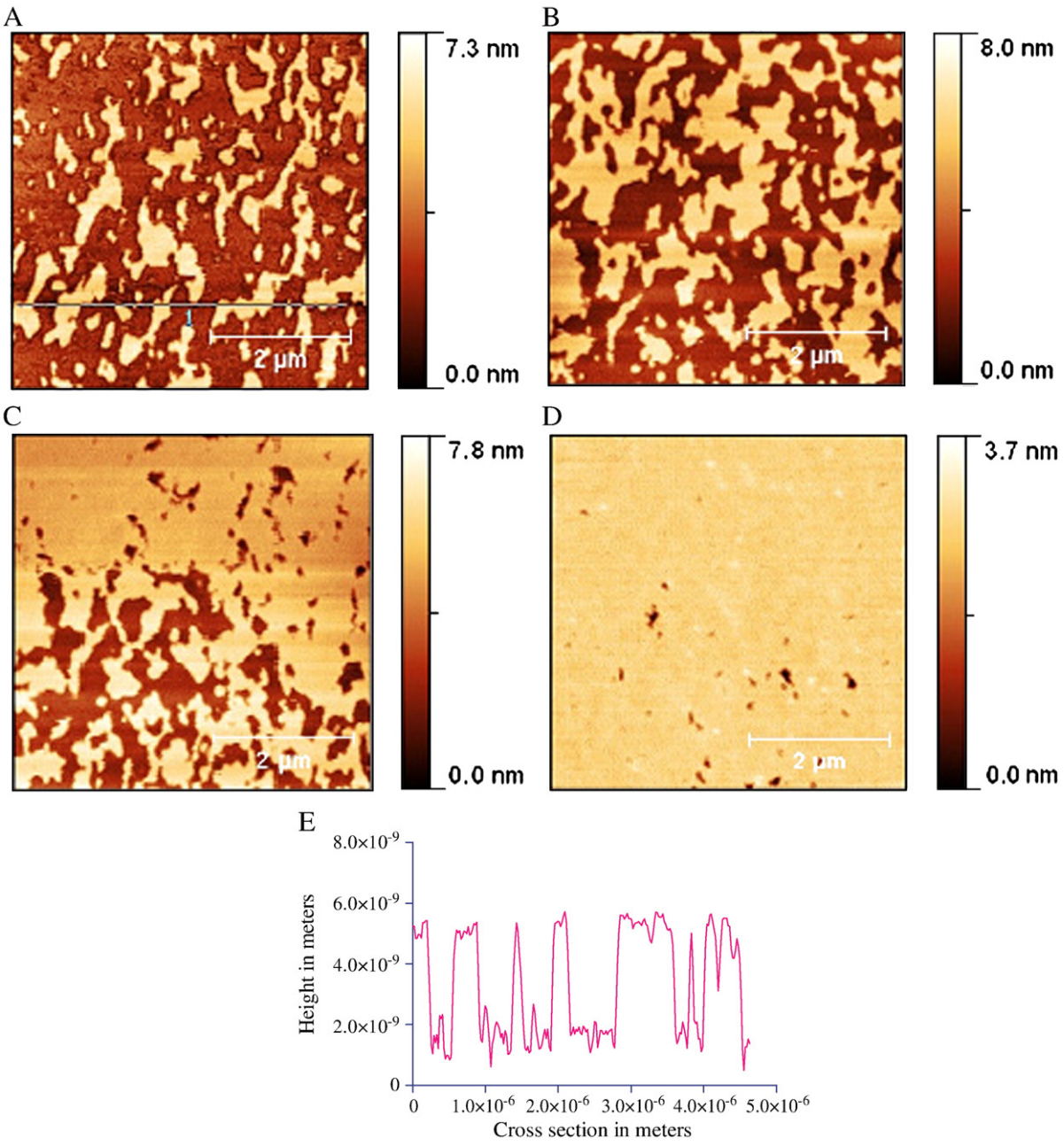

Fig. 3. Formation of a SCL bilayer on AHS surface. The data were collected (A) 5 min, (B) 30 min, (C) 60 min, (D) 70 min after placement of SCLLs on the AHS surface. (E) Profile of the cross section made in Fig. 3A.

temperature (Fig. 6), suggesting that the increase of positive charge in the Posintro™ nanoparticles and increased temperature promote the entropic part of the reaction. However, the Gibbs free energy does not have a clear dependence on any of these parameters, suggesting that the ubiquitous phenomenon of enthalpy-entropy compensation [28–30] is valid for this system as well (Table 2).

Although the fitting of the ITC data using the classic binding approach produced good results, a more intuitive description of the system was attempted. The individual components of the Posintro™ nanoparticles or SCLLs (*i.e.* lipids and Quil A) are neither free in solution nor the independent reactants. They are a part of strictly defined systems and thus it would be more appropriate to consider them as such. In other words, the binding reaction should be described as a function of molar concentration of particles, not the molar concentration of their components.

The fitting of the titration data using molar concentrations of the particles is shown in Fig. 5A, whereas the obtained thermodynamic parameters are reported in Table 3. The concentrations of the particles were calculated as described in the methodology section and fitted to the model of identical independent binding sites. Since every particle/liposome contains about 10^4–10^6 individual molecules, concentrations of the particles are extremely low (see Section 3.2), which results in very high values for the enthalpy and the binding constant.

The average value of Posintro™ nanoparticles bound per liposome is 24 (Table 3). To evaluate if this number is feasible, the surface area of a liposome ($4\pi r_{lipo}^2$), 5.0×10^{-14} m^2 was compared to the cross sectional area of a nanoparticle (πr_{nano}^2), 1.7×10^{-15} m^2. The ratio between the two, approximately 30, shows that more than the 24 nanoparticles can fit on the surface of a liposome, without experiencing steric constraints.

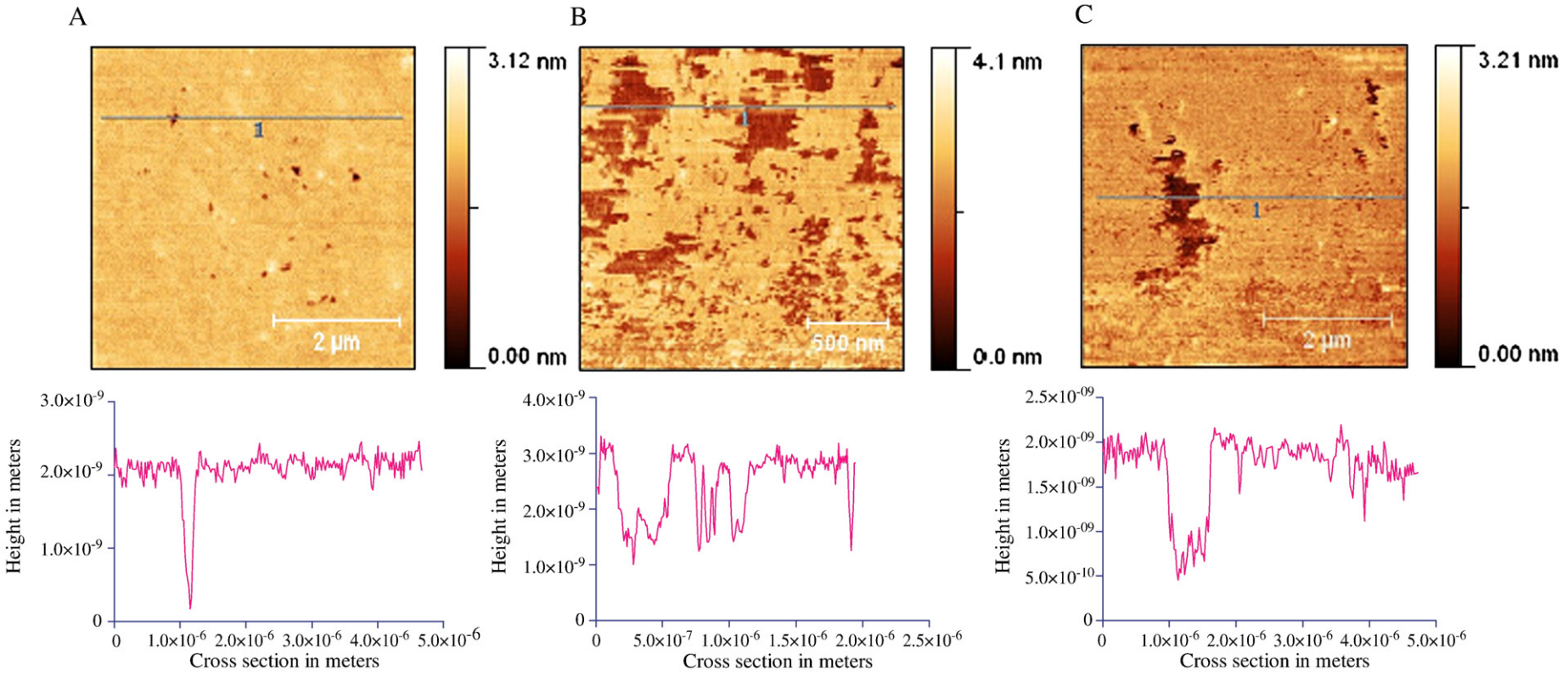

Fig. 4. AFM images of the AHS surface with SCL bilayer (A) before and (B and C) after (B, 15 min; C, 60 min) application of Posintro™ nanoparticles.

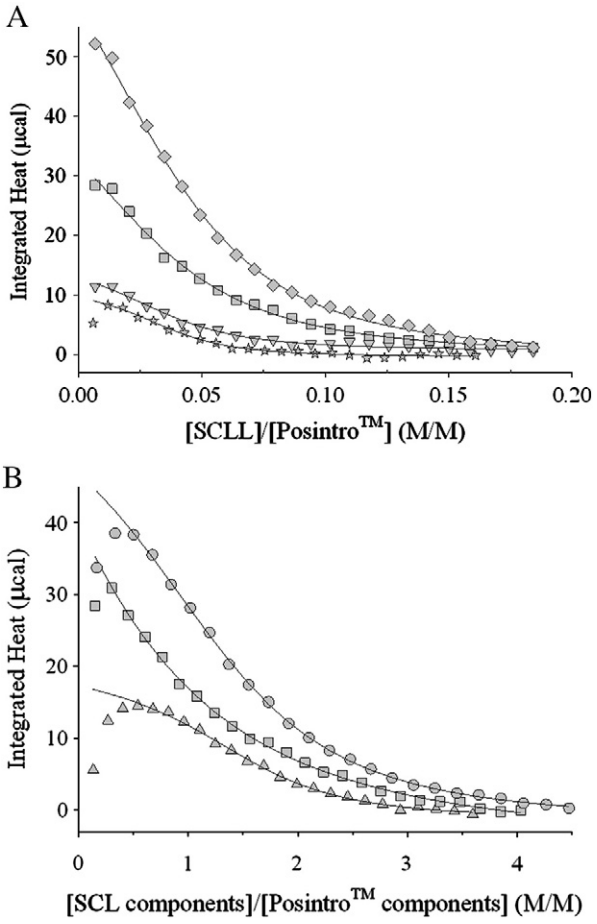

Fig. 5. Titration data describing interaction of SCLL with different types of Posintro™ at different temperatures. (A) Binding isotherms of SCLL to Posintro™ 25% nanoparticles at 5 °C, (stars); 15 °C, (down triangles), 25 °C, (squares), and 37 °C, (rhomb). The *x*-axis indicates a molar ratio between the number of SCLLs and Posintro™ nanoparticles (see text for details). The solid lines are the fitting curves with the parameters reported in Table 3. (B) Binding isotherms of SCL to Posintro™ 0% (up triangles), Posintro™ 25% (squares) and Posintro™ 50% (circles) at 25 °C. The injection heat is plotted against the total molar concentration ratio between SCL components (sum of concentrations of ceramides, cholesterols and fatty acids) and Posintro™ components (sum of concentrations of Quil A, POPC and cholesterol). Solid lines are fitting curves of the data using the parameters reported in Table 2. The two curves in panels A and B labelled with squares show two replicates of the same experiment.

3.5. Electrochemical Impedance Spectroscopy

Fitting the data to different equivalent circuits showed that an equivalent circuit with a resistor in series with a resistor–constant phase element resulted in the best fit of all data (Fig. 7). The first resistor (R_u) corresponds to the resistance of the electrodes and electrolyte whereas R_p is the resistance of the lipid bilayer and CPE is a constant phase element of the lipid layer on the electrode, where Y_0 and α represents the capacitive and exponential terms of the CPE, respectively. Change in the membrane resistance occurs when the rate of ion diffusion through the bilayer (*i.e.* leakiness of the membrane) changes. Change in the capacitive term of the CPE indicates a change in membrane thickness while the exponential term is affected by the membrane homogeneity.

After exposure to the various Posintro™ nanoparticles, the resistance of the lipid layer changed (Fig. 8), whereas the CPE parameters changed only slightly (data not shown). This means that the leakiness of the membrane seemed to change upon interaction, whereas neither the membrane thickness nor the homogeneity changed significantly. Exposure to DOPE/CHEMS-liposomes and to PBS pH 7.4 resulted in only minor changes in the resistance and the CPE of the membrane. The changes in membrane resistance were dependent on the concentration of DC-cholesterol in the Posintro™ nanoparticles (Fig. 8). Even though variations between the single measurements were observed, the tendency was that the resistance increased upon interaction with Posintro™ nanoparticles with no DC-cholesterol. This indicated that the ion diffusion through the bilayer decreased upon interaction. On the other hand, the resistance seemed to decrease upon interaction between Posintro™ 50% and the SCL bilayer, indicating that ion current through the lipid bilayer increased.

Table 2
Thermodynamic parameters of the interaction of various Posintro™ nanoparticles and DOPE/CHEMS liposomes with SCLL. The number of binding sites was floated in a limited region, where the upper limit was set to 2.

Posintro™	*T* (°C)	n	ΔH[a] (cal/mol)	k[a] (10^3 M^{-1})	ΔG[a] (kcal/mol)	ΔS[a] (cal/(K·mol))
0%	5	1.5	22	2.5	−4.3	15.6
	15	2.0/2.0	114/378	3.8/2.5	−4.7/−4.5	16.7/16.9
	25	0.6	290	10.6	−5.5	19.0
	37	2.0/2.0	839/1114	1.1/0.5	−4.3/−3.8	16.6/15.9
25%	5	1.1	99	7.6	−4.9	18.1
	15	2.0/1.3	293/117	1.9/4.6	−4.3/−4.8	16.0/17.1
	25	2.0/1.6	878/501	0.6/0.7	−3.7/−3.9	15.6/14.8
	37	0.7/1.1	741/734	4.2/0.6	−5.1/−3.8	18.9/15.0
50%	5	0.9	296	3.9	−4.6	17.5
	15	1.6/1.7	495/318	1.9/0.7	−4.3/−3.7	16.7/14.1
	25	0.7/1.0	661/776	3.3/5.7	−4.8/−5.1	18.3/19.8
	37	0.8/0.6	1116/1636	3.7/4.3	−5.1/−5.2	19.9/21.9
DOPE/CHEMS	25	5.2	663	0.38	−3.5	14.0

[a] Numbers stated as single values of "measurement 1"/"measurement 2".

3.6. Image analysis of the ITC samples

Cryo-TEM studies were performed to visualize the reaction observed by ITC. The images of SCLLs showed a spherical shape with an average diameter close to 100 nm (Fig. 9A), which correlated well with the DLS measurements. The Posintro™ nanoparticles appeared as cage-like structures (as previously described) with an average size of around 50 nm (Fig. 9B–D). Variations in surface charge affected the localization of the nanoparticles as increasing amounts of DC-cholesterol increased the attraction of the nanoparticles to the negatively charged lacey carbon film of the copper grids (Fig. 9B–D).

The appearance of the mixtures of Posintro™ nanoparticles and SCLLs 20 min after mixing varied with changes in the surface charge of the Posintro™ nanoparticles. For example, mixing Posintro™ 0% nanoparticles and SCLLs did not change the appearance of either component (Fig. 9E). Mixing Posintro™ 25% and SCLLs, on the other hand, resulted in non-spherical liposomes and increased appearance of spirals in the Posintro™ nanoparticle suspension (Fig. 9F). Finally,

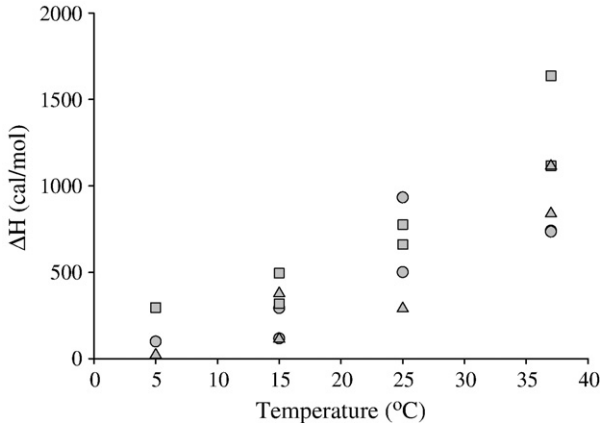

Fig. 6. Enthalpy of interaction between SCLL liposomes and Posintro™ nanoparticles with 0% (triangles), 25%, (squares) and 50%, (circles) DC-cholesterol.

Table 3
Thermodynamic parameters for the interaction between Posintro™ 25% and SCLL, when the fitting was done using the molar concentration of particles and liposomes.

T (°C)	n	ΔH (kcal/mol)	K (10^6 M)	ΔG (kcal/mol)	ΔS (cal/(K·mol))
5	28	1371	106	−10.2	41
15	24±3	3425/1617[a]	65/53	−10.4/−10.2	47/41
25	25±2	10076/5644	30/18	−10.3/9.9	67/53
37	19±4	10154/9698	69/39	−12.1/11.7	67/67

[a] Numbers stated as single values of "measurement 1"/"measurement 2".

mixing Posintro™ 50% and SCLLs resulted in destruction of the SCLLs, which can be seen as pieces of ruptured lipid membranes, and altered Posintro™ structure (Fig. 9G). Comparing the results, decreasing numbers of intact SCLLs and Posintro™ nanoparticles were observed with increasing percentage of DC-cholesterol. The damage inflicted by the Posintro™ 50% nanoparticles on SCLLs was time dependent as complete disintegration of the nanoparticle/liposome mixtures was observed 24 h after mixing (data not shown).

4. Discussion

The objective of the current study was to investigate the interaction between Posintro™ nanoparticles and SCL liposomes and bilayers in order to elucidate the mechanism of penetration into the intercorneocyte space of the stratum corneum. The influence of the net surface charge was assessed by varying the percentage of DC-cholesterol in the Posintro™ nanoparticles.

4.1. Interaction of the Posintro™ nanoparticles with SCLLs

The initial FRET studies confirm an interaction between the nanoparticles and the liposomes as the donor fluorescence increases upon mixing of Posintro™ nanoparticles with SCLLs. Furthermore, the increase in fluorescence is the largest for the nanoparticles with the highest percentage of DC-cholesterol. This shows that the donor probe becomes more separated from the acceptor probe (both imbedded in SCLLs) as a result of the interaction with the Posintro™ nanoparticles, which suggests fusion of the nanoparticles with SCLLs or disruption of the liposomes.

Similarly, the changes in the membrane resistance correlate with the concentration of the positively charged DC-cholesterol. The EIS experiments show increased resistance of the SCL bilayer upon exposure to Posintro™ nanoparticles without DC-cholesterol, indicating that the interaction rendered the lipid bilayer denser. In contrast, exposure to Posintro™ 50% nanoparticles decreased the resistance of the lipid bilayer, indicating that in this case the lipid bilayer becomes less compact [31,32], which would happen if the bilayer was destructed, allowing the ions in the solution to freely pass through. The zeta potential is significantly lower for Posintro™ 50% nanoparticles than for the other Posintro™ nanoparticles (Table 1).

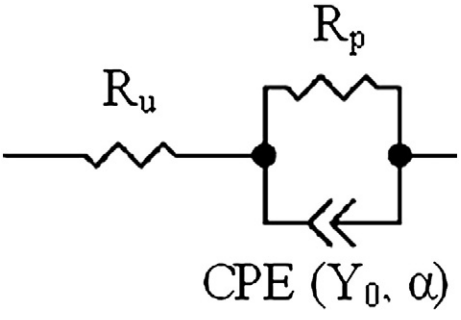

Fig. 7. Equivalent electrical circuit used for fitting the EIS data. R_u corresponds to the resistance of the electrodes and electrolyte whereas R_p is the resistance of the lipid bilayer. Y_0 and α represent the capacitive and exponential terms of constant phase element (CPE) of the lipid layer on the electrode, respectively.

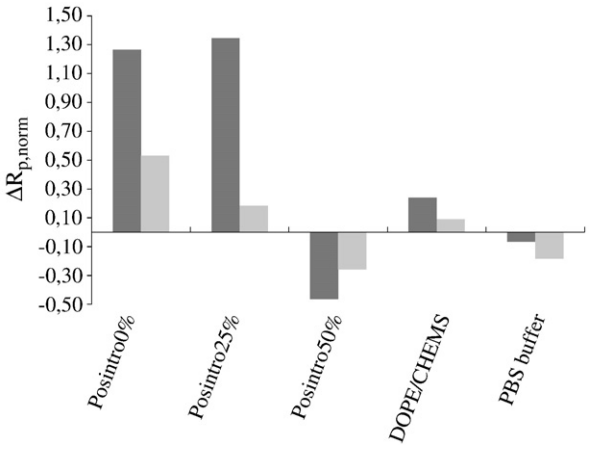

Fig. 8. Normalized change in the resistance of the lipid bilayer after exposure to Posintro™ nanoparticles with different content of DC-cholesterol (0%, 25%, 50%), DOPE/CHEMS liposomes, and PBS buffer at pH 7.4. Each column shows one single measurement.

This results in decreased electrostatic repulsion between the Posintro 50% nanoparticles and the lipid bilayer.

4.2. Energetics of the interaction

The enthalpy of interaction between Posintro™ nanoparticles and SCLLs is positive for all types of nanoparticles, suggesting that variation of the overall charge of the Posintro™ nanoparticles does not eliminate the entropy-driven character of the reaction. Both the low positive enthalpy and the weak association constant (Table 2) suggest that the binding does not involve specific interactions such as hydrogen or ionic bonds. In addition, the reaction occurs in spite of the fact that both reacting particles are negatively charged, indicating that the complex formation is driven by the hydrophobic effect. Not supporting this theory is, however, an experimental observation that association of the water-exposed hydrophobic surfaces results in a negative heat capacity change [30,33], whereas interaction between the Posintro™ nanoparticles and SCLLs has a positive ΔC_p (Fig. 6).

One feasible explanation that combines the observed features is that the reaction between the nanoparticles and the liposomes involves reorganization of the lipids of both components with possible lipid exchange between the two. The cryo-TEM images show that Posintro™ nanoparticles containing DC-cholesterol decrease the spherical shape of the SCLLs, suggesting that the packing of the lipids in liposomes is influenced by the nanoparticles. The poor packing of the hydrophobic tails indicated by the appearance of SCLLs with faceted surface (Fig. 9F–G) agrees well with the increased disorder, and thus the elevated mobility of lipids upon interaction. This process is similar to the case of melting transitions of solids, where both the enthalpy and the heat capacity are positive.

It should be noted that the binding models used for the data interpretation imply the reversibility of the binding reactions, whereas association of nanoparticles and liposomes is not completely reversible—a presence of irreversible processes is obvious from the cryo-TEM images, showing disruption of the liposomes and complete disintegration with time (only observed for Posintro™ 50%). However, the latter reaction occurs on a time-scale exceeding the duration of the ITC experiment. The effect from the binding is measured within 2–4 min (the time for the baseline to reach equilibrium level upon injection), whereas the effect of the irreversible process (caught in the images) is observed after 20 min. Therefore, interpretation of the titration experiments concerns only the short time-scale association reaction and ignores the contribution from the long-term irreversible processes.

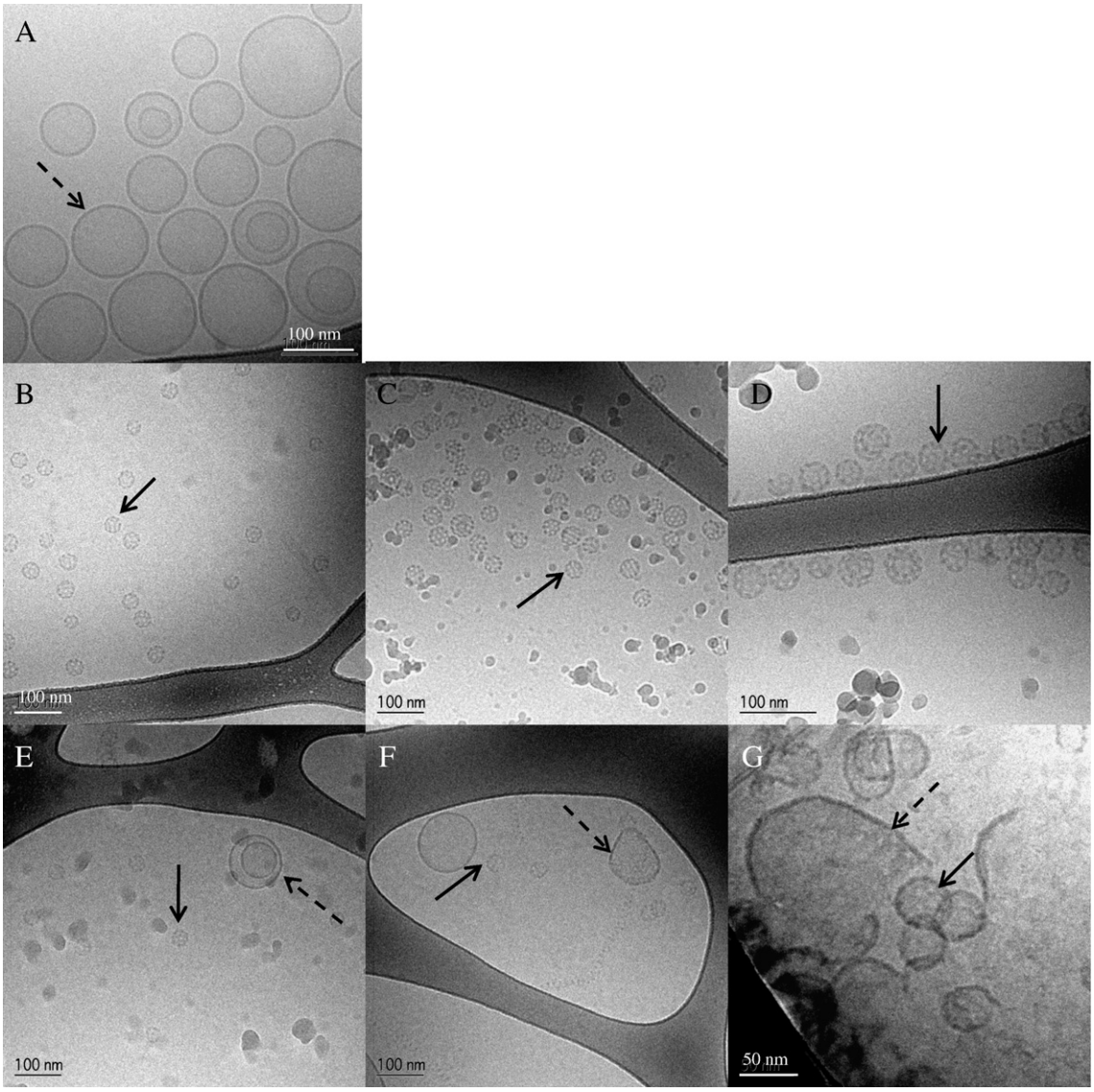

Fig. 9. Cryo-TEM images of SCLLs, Posintro™ nanoparticles and the titration products of the two. (A) 10 mM SCLL liposomes alone, (B) Posintro™ 0% nanoparticles, (C) Posintro™ 25% nanoparticles, (D) Posintro™ 50% nanoparticles. (E) Mixture of Posintro™ 0% and SCLLs after titration. (F) Mixture of Posintro 25% nanoparticles and SCLLs after titration. (G) Mixture of Posintro™ 50% and SCLLs after titration. Black arrow: Posintro™ nanoparticles, dashed black arrow: SCLLs

The Gibbs free energy of association between SCLLs and Posintro™ nanoparticles does not show a clear correlation to either the experimental temperature or the amount of DC-cholesterol. However, examination of the cryo-TEM images (Fig. 9E–G) shows that the liposomes become affected the most by the Posintro™ nanoparticles with the highest percentage of DC-cholesterol. The images also show that the damage to the liposomes, and hence the irreversibility of the interaction, worsen upon increase in the amount of DC-cholesterol. Therefore, the liposome destruction might be associated with such changes in ΔG that oppose the binding and diminish the overall free energy effect of the interaction.

4.3. Mechanism of penetration into the skin

The current investigation was initiated as a follow up on previous studies [14], from which we hypothesize that the Posintro™ nanoparticles disturb the intercellular lipid lamellae in the stratum corneum and thereby enhance the penetration of other compounds. In those studies, it was observed that the Posintro™ nanoparticles seemed to penetrate into the stratum corneum through the intercellular space. Based on these observations, a model system of lipids in the intercorneocyte space in the stratum corneum was investigated. However, only assumptions can be made about the potential penetration mechanism through stratum corneum; as other aspects, which are not present in this model, also interfere with penetration of drugs. For example, stratum corneum has, besides the intercellular lipid bilayers, the keratinocytes, which can interfere with the penetration of drugs. Also, other routes of penetration can contribute to the uptake of the drugs and delivery system. Moreover, the hydration of SCLLs is different than that of the intercellular lipids.

The increased concentrations of DC-cholesterol are expected to increase the penetration through the skin, as the barrier function of the skin is reduced upon destruction of the intercorneocyte matrix. If this is the case for antigens attached to Posintro™ nanoparticles, increasing amounts of DC-cholesterol would result in increased delivery of antigen across the skin.

In conclusion, the results of fluorescence and the cryo-TEM studies suggest increased destruction of SCLLs with increasing concentrations of DC-cholesterol, whereas the ITC reports an increasingly entropy-driven process. Interpolating these conclusions to the skin lipids, means that the intercorneocyte matrix found in the stratum corneum would be more affected/damaged by the Posintro™ nanoparticles

with the higher percentage of DC-cholesterol. Possibly, this interaction leads to a partial destruction of the penetrating particles [15], a hypothesis supported by the cryo-TEM studies. This finding confirms the current belief that the Posintro™ nanoparticles are too big to squeeze through the <20 nm passage [8] between the corneocytes as intact particles [14], which in turn indicates that the nanoparticles are broken down as a result of their interaction with the stratum corneum lipids and that the mechanism of their penetration into the skin involves their fusion with the stratum corneum.

Acknowledgments

This study was financially supported by the Danish National Advanced Technology Foundation (HBM, purchase of ITC), Drug Research Academy, and Ministry of Science, Technology and Innovation (MRK). We thank Svetlana V. Yevchenko from Nordic Vaccine A/S for the HP-TLC analysis and Peter Vittrup from Aalborg University for helpful guidance with the charge determinations. We also thank Gunnel Karlsson at Biomicroscopy Unit, Polymer and Materials Chemistry, Chemical Centre, Lund University, Lund, Sweden for help with the cryo-TEM work.

References

[1] I.G. Barr, G.F. Mitchell, ISCOMs (immunostimulating complexes): the first decade, Immunol. Cell Biol. 74 (1996) 8.
[2] W.T. McBurney, D.G. Lendemans, J. Myschik, T. Hennessy, T. Rades, S. Hook, In vivo activity of cationic immune stimulating complexes (PLUSCOMs), Vaccine (2008).
[3] D.G. Lendemans, J. Myschik, S. Hook, T. Rades, Cationic cage-like complexes formed by DC-cholesterol, Quil-A, and phospholipid, J. Pharm. Sci. 94 (2005) 1794.
[4] N. Kirkby, K. Dalsgaard, Polynucleotide Binding Complexes Comprising Sterols and Saponins, 2002.
[5] N. Kirkby, P. Samuelsen, Composition for Vaccination, 2006.
[6] C.M. Huang, Topical vaccination: the skin as a unique portal to adaptive immune responses, Semin. Immunopathol. 29 (2007) 71.
[7] L.C. Zaba, J.G. Krueger, M.A. Lowes, Resident and "inflammatory" dendritic cells in human skin, J. Invest. Dermatol. 129 (2009) 302.
[8] P.W. Wertz, D.T. Downing, Stratum Corneum: Biological and Biochemical Considerations, in: J. Hadgraft, R.H. Guy (Eds.), Transdermal Drug Delivery, Marcel Dekker, New York, 1989, pp. 1–17.
[9] M.W. de Jager, G.S. Gooris, M. Ponec, J.A. Bouwstra, Lipid mixtures prepared with well-defined synthetic ceramides closely mimic the unique stratum corneum lipid phase behavior, J. Lipid Res. 46 (2005) 2649.
[10] M.W. de Jager, G.S. Gooris, I.P. Dolbnya, W. Bras, M. Ponec, J.A. Bouwstra, Novel lipid mixtures based on synthetic ceramides reproduce the unique stratum corneum lipid organization, J. Lipid Res. 45 (2004) 923.
[11] J.A. Bouwstra, P.L. Honeywell-Nguyen, G.S. Gooris, M. Ponec, Structure of the skin barrier and its modulation by vesicular formulations, Prog. Lipid Res. 42 (2003) 1.
[12] J.A. Bouwstra, P.L. Honeywell-Nguyen, Skin structure and mode of action of vesicles, Adv. Drug Deliv. Rev. 54 (Suppl 1) (2002) S41–S55.
[13] B.Y. Schuetz, A. Naik, R.H. Guy, Y.N. Kalia, Emerging strategies for the transdermal delivery of peptide and protein drugs, Expert Opin. Drug Deliv. 2 (2005) 533.
[14] H.B. Madsen, P. Ifversen, F. Madsen, B. Brodin, I. Hausser, H.M. Nielsen, In vitro cutaneous application of ISCOMs on human skin enhances delivery of hydrophobic model compounds through the stratum corneum, AAPS J. 11 (2009) 728.
[15] M. Kirjavainen, A. Urtti, I. Jaaskelainen, T.M. Suhonen, P. Paronen, R. Valjakka-Koskela, J. Kiesvaara, J. Monkkonen, Interaction of liposomes with human skin in vitro—the influence of lipid composition and structure, Biochim. Biophys. Acta 1304 (1996) 179.
[16] M. Kirjavainen, A. Urtti, R. Valjakka-Koskela, J. Kiesvaara, J. Monkkonen, Liposome-skin interactions and their effects on the skin permeation of drugs, Eur. J. Pharm. Sci. 7 (1999) 279.
[17] S. Hoglund, K. Dalsgaard, K. Lovgren, B. Sundquist, A. Osterhaus, B. Morein, ISCOMs and immunostimulation with viral antigens, Subcell. Biochem. 15 (1989) 39.
[18] L.H. Mikkelsen, Applications and limitations of the colloid titration method for measuring activated sludge surface charges, Water Res. 37 (2003) 2458.
[19] M.L. Christensen, M. Hjorth, K. Keiding, Characterization of pig slurry with reference to flocculation and separation, Water Res. 43 (2009) 773.
[20] A.D. Bangham, R.W. Horne, A.M. Glauert, J.T. Dingle, J.A. Lucy, Action of saponin on biological cell membranes, Nature 196 (1962) 952.
[21] D. Handloser, V. Widmer, E. Reich, Separation of Phospholipids by HPTLC - An Investigation of Important Parameters, J. Liquid Chromatogr. Relat. Technol. 31 (2008) 1857.
[22] J. Thurin, M. Thurin, M. Herlyn, D.E. Elder, Z. Steplewski, W.H. Clark, H. Koprowski, Gd2 ganglioside biosynthesis is a distinct biochemical event in human-melanoma tumor progression, FEBS Lett. 208 (1986) 17.
[23] K. Dalsgaard, Thinlayer chromatographic fingerprinting of commercially available saponins, Dan. Tidsskr. Farm. 44 (1970) 327.
[24] N. Duzgunes, J.A. Goldstein, D.S. Friend, P.L. Felgner, Fusion of liposomes containing a novel cationic lipid, N-[2, 3-(dioleyloxy)propyl]-*N,N,N*-trimethylammonium: induction by multivalent anions and asymmetric fusion with acidic phospholipid vesicles, Biochemistry 28 (1989) 9179.
[25] N. Kucerka, M.A. Kiselev, P. Balgavy, Determination of bilayer thickness and lipid surface area in unilamellar dimyristoylphosphatidylcholine vesicles from small-angle neutron scattering curves: a comparison of evaluation methods, Eur. Biophys. J. 33 (2004) 328.
[26] T. Jain, J. Básti, T. Hansen, N. Larsen, R. Taboryski, and N. Rozlosnik, Characterization of PEDOT-tosylate Microelectrodes for Biosensor Applications, Biosens. Bioelectron. (Submitted for publication).
[27] N. Rozlosnik, New directions in medical biosensors employing poly(3,4-ethylenedioxy thiophene) derivative-based electrodes, Anal. Bioanal. Chem. 395 (3) (2009) 637.
[28] A. Cooper, Thermodynamic analysis of biomolecular interactions, Curr. Opin. Chem. Biol. 3 (1999) 557.
[29] E. Gallicchio, M.M. Kubo, R.M. Levy, Entropy-enthalpy compensation in solvation and ligand binding revisited, J. Am. Chem. Soc. 120 (1998) 4526.
[30] K. Sharp, Entropy-enthalpy compensation: Fact or artifact? Protein Sci. 10 (2001) 661.
[31] W.K. Chang, W.C. Wimley, P.C. Searson, K. Hristova, M. Merzlyakov, Characterization of antimicrobial peptide activity by electrochemical impedance spectroscopy, Biochim. Biophys. Acta 1778 (2008) 2430.
[32] F. Yang, X. Cui, X. Yang, Interaction of low-molecular-weight chitosan with mimic membrane studied by electrochemical methods and surface plasmon resonance, Biophys. Chem. 99 (2002) 99.
[33] P.L. Privalov, S.J. Gill, Stability of protein structure and hydrophobic interaction, Adv. Protein Chem. 39 (1988) 191.